

UNCLASSIFIED

AD NUMBER

AD473662

LIMITATION CHANGES

TO:

Approved for public release; distribution is unlimited.

FROM:

Distribution authorized to U.S. Gov't. agencies and their contractors;
Administrative/Operational Use; NOV 1965. Other requests shall be referred to Air Force Arnold Engineering Development Center, Arnold AFB, TN.

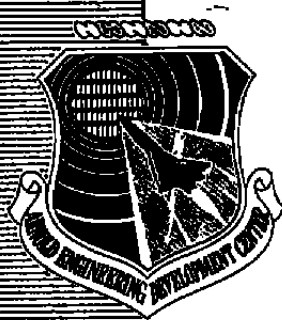
AUTHORITY

aedc ltr, 2 aug 1966

THIS PAGE IS UNCLASSIFIED

Wingman

DOC NUM SER CN
UNC00755-PDC A 1



**MEASUREMENT OF ELECTRICAL CONDUCTIVITY
IN A LOW-DENSITY SUPERSONIC
PLASMA**

J. A. Sprouse
ARO, Inc.

November 1965

**ROCKET TEST FACILITY
ARNOLD ENGINEERING DEVELOPMENT CENTER
AIR FORCE SYSTEMS COMMAND
ARNOLD AIR FORCE STATION, TENNESSEE**

NOTICES

When U. S. Government drawings specifications, or other data are used for any purpose other than a definitely related Government procurement operation, the Government thereby incurs no responsibility nor any obligation whatsoever, and the fact that the Government may have formulated, furnished, or in any way supplied the said drawings, specifications, or other data, is not to be regarded by implication or otherwise, or in any manner licensing the holder or any other person or corporation, or conveying any rights or permission to manufacture, use, or sell any patented invention that may in any way be related thereto.

Qualified users may obtain copies of this report from the Defense Documentation Center.

References to named commercial products in this report are not to be considered in any sense as an endorsement of the product by the United States Air Force or the Government.

MEASUREMENT OF ELECTRICAL CONDUCTIVITY
IN A LOW-DENSITY SUPERSONIC
PLASMA

J. A. Sprouse
ARO, Inc.

FOREWORD

The work reported herein was sponsored by Arnold Engineering Development Center (AEDC), Air Force Systems Command (AFSC), Arnold Air Force Station, Tennessee under Program Element 61445014, Project 8951, Task 895101.

The results of research presented were obtained by ARO, Inc. (a subsidiary of Sverdrup and Parcel, Inc.) in the Rocket Test Facility (RTF), Propulsion Research Area (R-2A5) under Contract AF40(600)-1200. The research was conducted under ARO Project No. RW3501, and the manuscript was submitted for publication on June 10, 1965 as partial results of this research effort.

The author wishes to acknowledge many rewarding and stimulating discussions held with W. K. McGregor (ARO, Inc.) during the course of this research. Also, thanks are due to G. E. Staats and J. Fröhlich (ARO, Inc.) for their contributions to the work presented in this report.

This technical report has been reviewed and is approved.

John R. Cureton
Captain, USAF
Gas Dynamics Division
DCS/Research

Donald R. Eastman, Jr.
DCS/Research

ABSTRACT

Electrical conductivities in the range from 70 to 280 mhos/meter were measured in an arc-heated, low-density, supersonic argon plasma. Measurements were made using a single layer coil acting as one branch of a tuned parallel circuit of a crystal-controlled oscillator operating at 5 mc/sec. Electromagnetic coupling between radio-frequency-excited coils and plasmas was examined, and the results are presented in terms of a nondimensional parameter, Q_s , which, for a particular coil, is a function only of the conductivity of the plasma surrounding the coil. Calculated conductivities using a combined form of the Spitzer-Härm and Chapman-Cowling equations for prescribed plasma conditions compare favorably with the measured results.

CONTENTS

	<u>Page</u>
ABSTRACT	iii
NOMENCLATURE	vi
I. INTRODUCTION	1
II. CRITERIA FOR A CONDUCTIVITY TRANSDUCER	1
III. RF-EXCITED COILS AS CONDUCTIVITY TRANSDUCERS	
3.1 Electromagnetic Coupling of Coil and Plasma.	3
3.2 Physical Description of a Probe	6
3.3 Essential Features of the Electrical Circuit	6
3.4 Coil and Circuit Design Criteria	8
IV. APPLICATION TO ARC-HEATED PLASMAS	
4.1 Description of Plasma	10
4.2 Calibration	10
4.3 Measurement Procedures	11
4.4 Results.	11
4.5 Comparison of Measured and Calculated Values of Plasma Conductivity	12
4.6 Discussion of the Measurements	13
V. SUMMARY	14
REFERENCES.	15
APPENDIX I - Hydromagnetic Effects	17

ILLUSTRATIONS

Figure

1. Cross-Sectional View of Coil and Probe Support	19
2. Oscillator and Probe	
a. Schematic Diagram of Crystal-Controlled Oscillator	20
b. A-C Equivalent Circuit of Oscillator for $C \leq C_0$	20
c. Plate Voltage, E_p , versus Capacitance, C	20
3. Schematic Diagram of Electrical Circuit Including Power Supply and Triggering Unit.	21
4. Oscillator Characteristics	
a. Recorded Output Voltage, E_p , (volts peak-to-peak)	22
b. Capacitance, C ($\mu\mu fd$)	22
c. D-C Plate Current (ma)	22

<u>Figure</u>	<u>Page</u>
5. Test Configurations	
a. Apparatus Schematic and Plasma Stream Characteristics	23
b. Free Jet Configuration with Dominant Flow Features Outlined	23
6. Calibration Curve, ΔE (volts peak-to-peak) versus σ (mhos/meter)	24
7. Plot of ΔE (volts peak-to-peak) versus Plasma Generator Input Power, P (kilowatts)	25
8. Plot of Plasma Conductivity, σ (mhos/meter) versus Plasma Generator Input Power, P (kilowatts)	26

NOMENCLATURE

A	$r_g/Q\omega L$
B	Magnetic field vector
C	Capacitance of parallel circuit
C₀	Capacitance of parallel circuit in free space at maximum plate voltage
C'₀	Capacitance of parallel circuit when coil is immersed in a conductive medium at maximum plate voltage
E	Electric field vector
E_g	Equivalent oscillator voltage
E_p	Plate voltage of oscillator
E_{p0}	Maximum plate voltage in free space
E'_{p0}	Maximum plate voltage in a conductive medium
G (Q_s)	$(Q_s^2 + 1)(Q_s^2 + k^2 Q Q_s + 1)/[1 + Q_s^2 (1 - k^2)]^2$
J	Current density vector
j	$\sqrt{-1}$
k	Coupling coefficient between coil and conductive medium
L	Inductance of coil in free space
L'	Inductance of coil in a conductive medium

L_s	Lumped equivalent inductance of the conductive medium
n_e	Electron number density
n_H	Plasma heavy particle number density
Q	$\omega L/R$
Q'	$\omega L'/R'$
Q_c	Electron-atom collision cross section
Q_s	$\omega L_s/R_s$
R	Internal resistance of coil in free space
R'	Internal resistance of coil in a conductive medium
R_s	Lumped equivalent resistance of the conductive medium
r_g	Equivalent internal resistance of oscillator
T_e	Electron temperature
W_d	Electromagnetic energy dissipated in one cycle
W_s	Electromagnetic energy stored
Z_p	Plate circuit impedance of parallel circuit
Z_{p_0}	Plate circuit impedance of parallel circuit when $C = C_0$
Z'_{p_0}	Plate circuit impedance of parallel circuit when $C = C'_0$
α	Degree of ionization
δ	Penetration depth
ϵ	Permittivity
μ	Permeability
σ	Conductivity
ω	Angular frequency

CONSTANTS

$$\epsilon_0 = 8.854 \times 10^{-12} \text{ farads/meter}$$

$$\mu_0 = 1.257 \times 10^{-6} \text{ henries/meter}$$

$$\pi = 3.1416$$

SECTION I INTRODUCTION

The design, analysis, and testing of plasma devices require a knowledge of the electrical conductivity of the working fluid. In the laboratory plasmas used for wind tunnel and other gas flow experiments, present knowledge does not allow reliable calculations of the conductivity; it must be measured.

This report is concerned with measurement of electrical conductivity and with application to a low-density, arc-heated supersonic plasma. It will be shown that the values of conductivity are in the same range as the calculated values, which were obtained by using measured electron temperatures in the classical equations. The content of the report is, however, more general in scope, and the method presented is applicable to the measurement of conductivity in any medium.

The electrical conductivity transducer found to be the most useful consists of a single layer coil, which acts as one arm of a tuned, parallel network in the plate circuit of a crystal-controlled oscillator operating at 5 mc/sec. Similar coils have been used by others, and extensive references are found describing both the theoretical aspects of the interaction of the electromagnetic field and the plasma (Ref. 1) and the more practical aspects of associated circuitry (Refs. 2 through 8). In the method presented herein, a direct relationship between the plate voltage and the conductivity of the medium is established with the plate voltage being the only required measurement. In this way, the measurement is simplified over other apparatus that have been reported. Also, the analysis of the problem and the transducer presented in this report leads to a clarification of certain aspects of conductivity measurements not adequately treated in the literature. Among these are the effect of dielectric constant of the medium on the measurements, the conditions under which the coupling between the plasma and the electromagnetic fields of the coil are predominantly conductivity dependent, and the uncertainty introduced by use of electrolytic solutions as the calibration medium.

SECTION II CRITERIA FOR A CONDUCTIVITY TRANSDUCER

The electrical properties of a linear-isotropic medium are completely specified by the four scalar parameters: σ (electrical conductivity), μ (permeability), ϵ (permittivity), and ρ (free charge density).

The net free charge in a plasma is zero except at a plasma-solid boundary. In particular, when a metal is exposed to a plasma, a positive charge density (sheath) accumulates at the metal-plasma interface. This sheath effect makes it virtually impossible to use plasma conductivity transducers which require direct contact between metals and the plasma.

One method of avoiding the difficulties associated with the sheath is to use radio-frequency (RF) excited coils since the coupling between the transducer and plasma is magnetic rather than direct. Direct computation of the conductivity from measurements using RF coils becomes extremely difficult since the conductivity is one of the three properties of the medium appearing as coefficients in the electromagnetic wave equation.

$$\left\{ \nabla^2 - \mu \sigma \frac{\partial}{\partial t} - \mu \epsilon \frac{\partial^2}{\partial t^2} \right\} \begin{Bmatrix} \mathbf{B} \\ \mathbf{E} \end{Bmatrix} = 0 \quad (1)$$

Appendix I contains a more complete form of the wave equation for a flowing ionized gas. It is shown that the hydromagnetic term can be neglected and that Eq. (1) is valid for supersonic plasmas.

From Eq. (1) it can be seen that when the fields are varying sinusoidal in time with an angular frequency, ω , and for the particular case, $\sigma \gg \omega \epsilon$, and $\mu = \mu_0$, then the wave equation can be replaced approximately by the diffusion equation as shown in Eq. (2).

$$\left\{ \nabla^2 - \mu_0 \sigma \frac{\partial}{\partial t} \right\} \begin{Bmatrix} \mathbf{B} \\ \mathbf{E} \end{Bmatrix} = 0 \quad (2)$$

Typical values of permittivity for electrolytic solutions and plasmas are $80 \epsilon_0$ and ϵ_0 , respectively (where $\epsilon_0 = 8.854 \times 10^{-12}$ farads/meter). For a frequency of 5 mc, the condition that $\sigma \gg \omega \epsilon$ is satisfied by two orders in magnitude for values of conductivity exceeding 2.5 mhos/meter in electrolytic solutions and 0.028 mho/meter in plasmas.

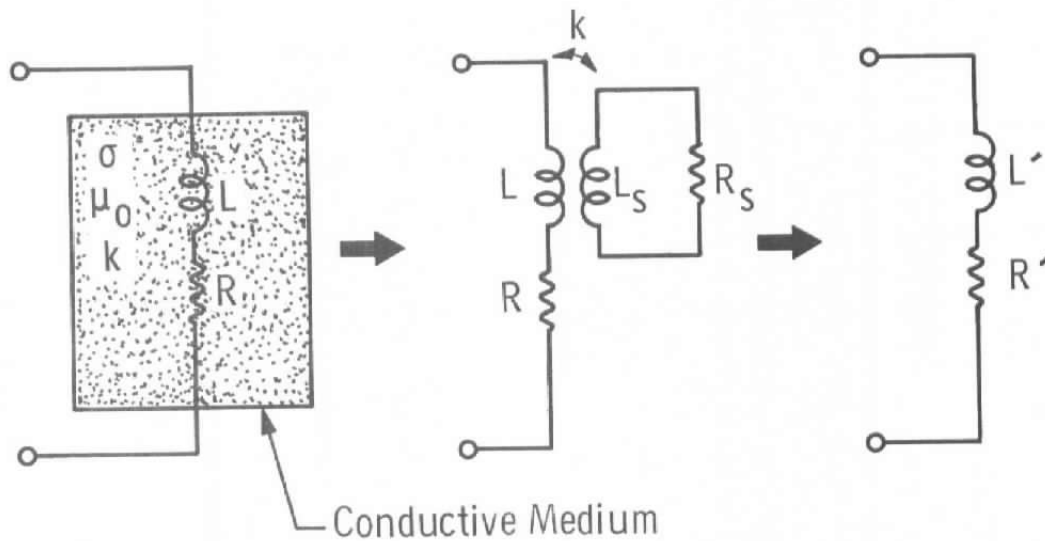
SECTION III RF-EXCITED COILS AS CONDUCTIVITY TRANSDUCERS

Various techniques and circuits have been developed which utilize coils to measure the conductivity of a plasma (Refs. 2 through 8). Most often a single layer coil is used in one branch of a parallel-tuned circuit, and the magnetic field distortion due to the presence of the plasma

is then related to the value of plasma conductivity. Whatever the circuit or means of detection, the field distortion results from "eddy currents" induced in the conductive medium by the time varying magnetic field.

3.1 ELECTROMAGNETIC COUPLING OF COIL AND PLASMA

One method of dealing with these eddy currents is to lump the distributed inductance and resistance associated with each closed-current path into a total equivalent inductance, L_s , and total equivalent resistance, R_s . Further, if it is assumed that the coil is inductively coupled to the conductive medium through a coupling coefficient, k , then the presence of the conductive medium can be examined by reflecting the lumped inductance and resistance into the coil, using ordinary transformer analysis. This procedure is schematically illustrated in Sketch 1.



Sketch 1

From this transformation a new value of coil inductance, L' , and resistance, R' , due to the presence of the conductive medium is obtained as a function of the coupling coefficient, k , total equivalent resistance, R_s , and total equivalent inductance, L_s .

Therefore,

$$L' = L \left[1 - \frac{k^2 (\omega L_s)^2}{R_s^2 + (\omega L_s)^2} \right] \quad (3)$$

$$R' = R \left[1 + \frac{k^2 (\omega L) (\omega L_s) R_s}{R [R_s^2 + (\omega L_s)^2]} \right] \quad (4)$$

If the nondimensional parameters, $Q = \omega L/R$, $Q' = \omega L'/R'$, and $Q_s = \omega L_s/R_s$, are substituted into Eqs. (3) and (4), then the following useful relationships are obtained:

$$\frac{L'}{L} = \frac{1 + Q_s^2 (1 - k^2)}{1 + Q_s^2} \leq 1 \quad (5)$$

$$\frac{R'}{R} = \frac{Q_s^2 - k^2 Q Q_s + 1}{1 + Q_s^2} \geq 1 \quad (6)$$

$$\frac{Q'}{Q} = \frac{1 + Q_s^2 (1 - k^2)}{Q_s^2 + k^2 Q Q_s + 1} \leq 1 \quad (7)$$

The equality signs on the right apply only when either Q_s or k are zero; otherwise, the inequality sign governs the relationship of the three ratios. From Eq. (6) it can be seen that the parameter, $k^2 Q$, appears as an amplifying factor; hence, to enhance the sensitivity of the system, this parameter should be made large. Ultimately, this means that the Q of the coil should be made large regardless of the circuit in which the coil is used.

For a given coil and excitation frequency, the coupling coefficient, k (which must always be less than or equal to unity), depends solely upon the geometry of the coil and the proximity of the coil and the conductive medium. The nondimensional parameter, Q_s , is more difficult to handle; however, it can be shown that this quantity for a given coil and excitation frequency is a function only of the conductivity of the surrounding medium. The proof of this latter statement can be shown by considering the basic definition of Q_s , which is given below by Eq. (8) (Ref. 9):

$$Q_s = 2\pi \left[\frac{\text{Electromagnetic Energy Stored in the Medium}}{\text{Electromagnetic Energy Dissipated in One Cycle}} \right] \quad (8)$$

The energy stored in the medium, W_s , is given by

$$W_s = \int_{vol} \left(\epsilon \mathbf{E} \cdot \mathbf{E} + \frac{\mathbf{B} \cdot \mathbf{B}}{\mu} \right) dv \quad (9)$$

It has been shown (Ref. 10) that the energy stored in the magnetic field is several orders of magnitude greater than the energy stored in the electric field for a coil whose dimensions are small compared to a wavelength. Thus, Eq. (9) reduces to

$$W_s \doteq \frac{1}{\mu} \int_{vol} \mathbf{B} \cdot \mathbf{B} dv \quad (10)$$

The energy dissipated in one cycle, W_d , is

$$W_d = \int_0^{\frac{2\pi}{\omega}} \left[\int_{vol} \mathbf{J} \cdot \mathbf{E} \, dv \right] dt \quad (11)$$

Substituting $\mathbf{J} = \sigma \mathbf{E}$ in Eq. (11) yields

$$W_d = \sigma \int_0^{\frac{2\pi}{\omega}} \left[\int_{vol} \mathbf{E} \cdot \mathbf{E} \, dv \right] dt \quad (12)$$

Thus, Eq. (8) can be written as

$$Q_s \doteq \frac{2\pi}{\mu\sigma} \frac{\int_{vol} \mathbf{B} \cdot \mathbf{B} \, dv}{\int_0^{\frac{2\pi}{\omega}} \left[\int_{vol} \mathbf{E} \cdot \mathbf{E} \, dv \right] dt} \quad (13)$$

For a given coil and excitation frequency, ω , it can be seen that solutions for \mathbf{B} and \mathbf{E} to Eq. (2) can be put in the form

$$\mathbf{B} = \mathbf{B}(r, \sigma) \exp(j\omega t) \quad (14)$$

$$\mathbf{E} = \mathbf{E}(r, \sigma) \exp(j\omega t) \quad (15)$$

where r is the position vector.

Then

$$\mathbf{B} \cdot \mathbf{B} = B(r, \sigma) B^*(r, \sigma) = B^2(r, \sigma) \quad (16)$$

and

$$\mathbf{E} \cdot \mathbf{E} = E(r, \sigma) E^*(r, \sigma) = E^2(r, \sigma) \quad (17)$$

Substituting Eqs. (16) and (17) into Eq. (13) and integrating the denominator over one cycle yields

$$Q_s \doteq \frac{\omega}{\mu\sigma} \frac{\int_{vol} B^2(r, \sigma) \, d r^3}{\int_0^{\frac{2\pi}{\omega}} E^2(r, \sigma) \, d r^3} \quad (18)$$

Since r is simply a variable of integration, then it follows that Q_s is a function only of the conductivity. That is

$$Q_s = Q_s(\sigma) \quad (19)$$

At this point, one has a sufficient set of equations in terms of measurable quantities, L , L' , R , and R' , and the quantity, Q_s , to

completely characterize the problem. That is, eliminating k from Eqs. (5) and (6) yields

$$Q_s = \omega \left[\frac{L - L'}{R' - R} \right] = Q_s(\sigma) \quad (20)$$

A large portion of the following sections is devoted to a method of making the necessary measurements to determine this relationship without having to seek solutions to the wave equation and, subsequently, to Eq. (8). The reasoning is simply that exact solutions to either Eq. (2) or Eq. (8) are extremely difficult (if not impossible) to obtain for a coil of finite length immersed in a conductive medium.

Another aspect which must be considered before the coil can be used successfully as a conductivity transducer is the penetration depth (skin depth) of the electric and magnetic field into the conductive medium. This aspect becomes increasingly important when boundary layers form at the surface of the body, such as the case when a supersonic gas flows over the body. A conservative measure of this depth is given approximately by the expression (Ref. 11),

$$\delta = \sqrt{\frac{2}{\omega \mu \sigma}} \quad (21)$$

With regard to the materials presented in this report, δ is always greater than one body diameter; hence penetration depth is no problem.

3.2 PHYSICAL DESCRIPTION OF A PROBE

The coil used in these experiments consisted of forty turns of AWG No. 22 enameled copper wire wound on a 0.7-cm-diam porcelain rod and housed in a 1-cm-diam (outside) pyrex tube. Four feet of RG62/u coaxial cable was used to remotely locate the coil from the oscillator circuit. The inductance of the coil was approximately 4×10^{-6} henries with a Q of 72 at 5 mc/sec. The coil and probe support are illustrated in Fig. 1.

3.3 ESSENTIAL FEATURES OF THE ELECTRICAL CIRCUIT

The schematic diagram of the oscillator and probe is shown in Fig. 2, and the circuit diagram is shown in Fig. 3. This particular crystal-controlled oscillator has the desirable feature that oscillation will occur only when the plate circuit is either real or inductive (Ref. 9).

The rms plate voltage, E_p , versus capacitance, C , for this oscillator is shown in Fig. 2c. Note that the plate voltage has a sharp maximum E_{p_0} at the point where the parallel tank circuit is real and decreases as the capacitance is further reduced. The value of capacitance at this maximum plate voltage, E_{p_0} , is C_0 and is given by Eq. (22) (i. e., when the plate circuit impedance is real).

$$C_0 = \frac{L}{R^2 + (\omega L)^2} \quad (22)$$

When $C \leq C_0$ the oscillator can be replaced by the equivalent circuit shown in Fig. 2b.

The impedance, Z_p , of the tank circuit is

$$Z_p = \frac{R + j\omega L [(1 - \omega^2 LC) - CR^2/L]}{(\omega CR)^2 + (1 - \omega^2 LC)^2} \quad (23)$$

and the rms plate voltage, E_p , is

$$E_p = \frac{E_g Z_p}{r_g + Z_p} \quad (24)$$

Consider now the case when $C = C_0$ and for $Q \gg 1$. Equations (23) and (24) become

$$Z_{p_0} = RQ^2 = \omega LQ \quad (25)$$

and

$$E_{p_0} = E_g \left[\frac{1}{1 + r_g/Q\omega L} \right] \quad (26)$$

When the coil is immersed in the plasma, R , Q , and L in Eqs. (25) and (26) can be replaced by R' , Q' , and L' (see Eqs. (5), (6), and (7)). Also, C must be adjusted to a new C'_0 in order to obtain the maximum plate voltage, E'_{p_0} . That is,

$$C'_0 = \frac{L'}{R'^2 + (\omega L')^2} \quad (27)$$

and

$$E'_{p_0} = E_g \left[\frac{1}{1 + r_g/Q'\omega L'} \right] \quad (28)$$

By substituting for Q' and L' from Eqs. (5) and (7), respectively, and making the following substitutions,

$$G(Q_s) = \frac{(Q_s^2 + 1)(Q_s^2 + k^2 Q Q_s + 1)}{[1 + Q_s^2(1 - k^2)]^2} \quad (29)$$

and

$$A = r_g/Q\omega L \quad (30)$$

then Eq. (28) becomes

$$E'_{p_0} = E_g \left[\frac{1}{1 + A G(Q_s)} \right] \quad (31)$$

The change in plate voltage, $\Delta E = E_{p_0} - E'_{p_0}$ from free space conditions to immersion in the plasma is

$$\Delta E = E_{p_0} - E'_{p_0} = E_g \left[\frac{1}{1 + A} - \frac{1}{1 + AG} \right] \quad (32)$$

From Eq. (32) it can be seen that the change in plate voltage, ΔE , is a function of A , E_g , and G where G is a function of Q_s . For a particular oscillator circuit, A and E_g are constants; for a given probe, k is a constant. The parameter, Q_s , depends solely upon the conductivity of the surrounding medium provided that $\sigma \gg \omega\epsilon$. Therefore, under these conditions, the change in plate voltage is a function of the conductivity of the surrounding medium. That is,

$$\Delta E = \Delta E(\sigma) \quad (33)$$

Since the functional relationship as shown in Eq. (33) cannot be obtained analytically, it is necessary to obtain a numerical relationship between ΔE and σ through calibrations with mediums of known conductivity.

3.4 COIL AND CIRCUIT DESIGN CRITERIA

Since there are many factors to consider in designing the proper coil for conductivity measurements, there can be no standard procedure to follow. However, there are a few general observations which apply to all situations. In particular, to obtain maximum power transfer to the coil, the constant, A , (see Eq. (30)) should be approximately equal to unity. Then

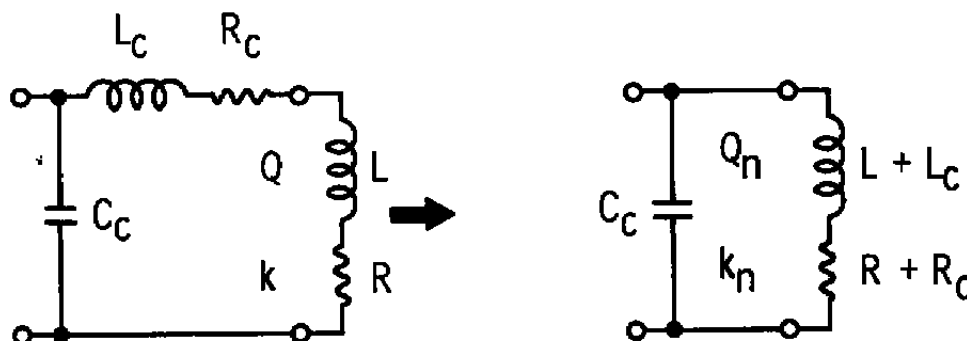
$$Q\omega L \doteq r_g \quad (34)$$

(For the circuit in this report, $r_g \doteq 7000$ ohms.)

The value of coil inductance, L , will depend upon coil dimensions and geometry which, in general, are peculiar to the particular application. The Q of a coil depends upon L and thus upon coil dimensions, and further, it depends upon such factors as wire size, spacing between adjacent turns, ratio of coil length to diameter, frequency, etc.; this makes it difficult to arrive at a preselected value of Q from basic principles. Criteria for designing a coil for a particular value of Q can be

found in the literature (Ref. 9). However, from experience, it has been found that a Q-meter is an invaluable aid in the trial and error selection of Q.

Another factor to consider in the design is the effects of using coaxial cable to remotely locate the coil from the oscillator. The length of coaxial cable should be kept to a minimum, and for operation at 5 mc or higher, lengths greater than 5 ft should be avoided. The coaxial cable has two adverse effects. First, it lowers the Q of the system, and, secondly, it lowers the coupling coefficient, k. This latter can be understood by noting that the coaxial cable introduces additional inductance and resistance in the branch without any additional coupling to the plasma. By treating the coaxial cable as lumped parameters as shown in Sketch 2 (this choice is used for convenience only), it can be shown that the coil can be replaced with a new coil and coupling coefficient, k_n .



Sketch 2

where

$$Q_n = \frac{\omega(L + L_c)}{R + R_c} \quad \text{and} \quad k_n = k \left(\frac{L}{L + L_c} \right)^{1/2}$$

Therefore, one must include the effects of coaxial cable when applying Eq. (34). Further, calibration must be made using the same type and length of coaxial cable as used in the test runs.

SECTION IV APPLICATIONS TO ARC-HEATED PLASMAS

The analysis of the coil and circuit presented in the previous sections shows that it is possible to make reliable measurements of plasma conductivity by using an RF-excited coil in conjunction with a crystal-controlled oscillator. In the following sections, measurements are presented, and these values are compared with calculated values using a combined form of the Chapman-Cowling and Spitzer-Härm equations.

4.1 DESCRIPTION OF PLASMA

The schematic diagram of the test cell, plasma generator, and plume geometry for normal operating conditions is shown in Fig. 5. The gas (argon) enters the arc-chamber and then expands through a 15-deg conical nozzle into a low-pressure test cell (0.3 to 0.5 mm Hg). The dominant flow features associated with this free jet configuration are schematically illustrated in Fig. 5b.

Typical values of Mach number, particle density, electron number density, and electron temperature at the nozzle exit are: Mach 5, 10^{15} atoms/cm³, 10^{13} electrons/cm³, and 7000°K, respectively.

4.2 CALIBRATION

Since the range of plasma conductivity of interest extends from a few mhos/meter to a few thousand mhos/meter, there is a problem in obtaining suitable calibration materials. The problem stems from the fact that only two classes of materials (excluding plasmas) have conductivities within the range of interest. These are: electrolytic solutions and properly prepared semiconductor materials. Ruling out semiconductors, for the present at least, due to cost and crystal size, leaves electrolytic solutions.

The calibration curve shown in Fig. 6 was obtained by immersing the coil in the following solutions and recording the change in output voltage: (a) normal solution of KCl, (b) saturated solution of NaCl, and (c) 0.5 normal solution of H₂SO₄. By varying the temperature of these solutions between 0 and 90°C, a range of conductivities from 6 to 165 mhos/meter is available (Ref. 12). The calibration curve may be in error because these published data were obtained by making voltage versus current measurements at a frequency of 1000 cps and applying Ohm's law. The errors may stem from two sources: First, the method assumes that a linear field exists within the medium, which may not be true, and that there are no sheath effects at the fluid-metal boundary. Second, the conductivity may be frequency dependent, and the measurements here were made at 5 mc. Thus, it is recognized that considerable research is required in this area in order to obtain an absolute calibration curve. Basically this problem arises from an attempt to correlate electromagnetic interactions at radio frequencies with massive ions having relatively large number densities and low mobilities to interactions with light electrons having lower number densities and higher mobilities.

Another factor that might appear to be of importance is that the electrolytic solutions have large values of permittivity ($\sim 85 \epsilon_0$), whereas the permittivity of plasmas is approximately that of free space ($\sim \epsilon_0$). However, as can be seen by Eqs. (2) and (13), permittivity is not a factor. The permeability is very nearly the same for both plasmas and electrolytic solutions ($\mu \sim \mu_0$) so that no effect would be expected. Both these facts are borne out in the experimental results.

4.3 MEASUREMENT PROCEDURES

Because of the high temperatures associated with the plasma, it was necessary to develop a measuring procedure which would significantly reduce the time that the transducer was immersed in the plasma.

With the technique described below, measurements in the plasma can be made in less than five seconds. This is accomplished by photographing the trace produced by the plate voltage, E_p , on an oscilloscope which is operating in the external triggering mode and at a sweep speed of 0.5 sec per division. By using an external trigger, it is possible to leave the shutter on the camera open. Then, by manually triggering the oscilloscope from the oscillator control panel (see Fig. 3) while tuning the capacitor about the value, C_0 (see Eq. (27)), a photograph appearing like the illustration in Fig. 4a is obtained. The maximum peak-to-peak output voltage is readily obtained from this illustration. It is a simple matter to determine when C is larger (smaller) than C_0 by observing the d-c plate current meter located on the oscillator panel. The current will abruptly increase (decrease) as C increases (decreases) past C_0 . This is illustrated in Fig. 4. It is expedient to obtain the calibration data in the same fashion.

4.4 RESULTS

The measurements reported herein were made at the exit of the nozzle and were obtained for gas flow rates of 1.37 and 2.37 gm/sec as the input power to the plasma generator was increased from 3 to 15 kw.

Since there is some doubt as to the values of conductivity of the electrolytic solutions, especially at radio frequencies, both the measured parameter, ΔE , and the corresponding values of σ , which were obtained from the calibration curve (see Fig. 6), are presented. Values of ΔE ranging from 42 to 65 volts peak-to-peak were recorded as the input power was increased from 3.5 to 15 kw and are shown in Fig. 7. Corresponding values of conductivity over this same range using the

calibration curve extend from 70 to 280 mhos/meter (see Fig. 8). These measured values are probably higher than those which truly exist since one would suspect that the conductivity of electrolytic solutions decreases with increasing frequency. This frequency effect would tend to shift the calibration curve shown in Fig. 6 to the left.

4.5 COMPARISON OF MEASURED AND CALCULATED VALUES OF PLASMA CONDUCTIVITY

In Table I values of degree of ionization, α , plasma conductivity, σ (mhos/meter), and electron density, $n_e = \alpha n_H$, are tabulated for electron temperatures, $T_e = 6000, 7000$, and 8000°K , and for heavy particle densities, $n_H = 10^{15}$ and $5 \times 10^{15} \text{ (cm}^{-3}\text{)}$. These values of electron temperatures and particle densities are characteristic of the plasma under consideration (Refs. 13 and 14).

TABLE I
TABULATED VALUES OF PLASMA CONDUCTIVITY USING A COMBINED FORM OF THE
CHAPMAN-COWLING AND SPITZER-HÄRM EQUATIONS FOR THREE VALUES OF
ELECTRON TEMPERATURE AND TWO VALUES OF HEAVY PARTICLE DENSITIES

T_e , $^\circ\text{K}$	$n_H = 1 \times 10^{15} \text{ cm}^{-3}$			$n_H = 5 \times 10^{15} \text{ cm}^{-3}$		
	α	n_e , cm^{-3}	σ , mhos meter	α	n_e , cm^{-3}	σ , mhos meter
6000	8.77×10^{-4}	8.77×10^{11}	9.8	3.92×10^{-4}	1.96×10^{12}	4.5
7000	8.93×10^{-3}	8.93×10^{12}	105.	3.99×10^{-3}	2×10^{13}	51
8000	6.6×10^{-2}	6.6×10^{13}	690.	2.95×10^{-2}	1.47×10^{14}	367

The degree of ionization, α , was obtained from Saha's equation using the electron temperature (Ref. 15).

The calculated values of conductivity were obtained by applying a combined form of the Chapman-Cowling equation and the Spitzer-Härm equation (Ref. 1). The Chapman-Cowling expression for plasma conductivity was developed by considering only short-range forces (slightly ionized gas), and the Spitzer-Härm equation evolved from treating a fully ionized plasma (long-range forces). Kantrowitz et al. (Ref. 16) suggested that, for an arbitrary degree of ionization, the two expressions can be combined to describe the effects between the two extremes. That is, as an electron moves through a plasma, two types of retarding forces, which are due to short-range and long-range encounters, inhibit the flow of electric current. Since these retarding forces act like resistances in series and because resistivity is essentially the reciprocal

of conductivity, then an expression for plasma conductivity for an arbitrary degree of ionization should be given by

$$\frac{1}{\sigma} = \frac{1}{\sigma_s} + \frac{1}{\sigma_c} \quad (35)$$

where σ_s is the conductivity calculated using the Spitzer-Härm equation and σ_c is the conductivity found using the Chapman-Cowling equation. For argon these equations are (Ref. 1)

$$\sigma_s = \frac{1.56 \times 10^{-2} T_e^{3/2}}{\ln [1.23 \times 10^4 T_e^{3/2} / n_e^{1/2}]} \text{ (mhos/meter)} \quad (36)$$

$$\sigma_c = 3.34 \times 10^{-10} \frac{a}{Q_c T_e^{1/2}} \text{ (mhos/meter)} \quad (37)$$

In these equations, n_e is in cm^{-3} , T_e in degrees Kelvin, and Q_c (electron-atom collision cross section) in cm^2 . Values for Q_c were taken from Massey-Burhop (Ref. 17).

4.6 DISCUSSION OF THE MEASUREMENTS

The purpose of including the above calculation in this report was to ensure that the measured values of conductivity are in the same range as those predicted theoretically. The theoretical calculations suffer from a lack of knowledge of the true form of the equations and uncertain data, such as the collision cross section, Q_c . The calculated values are only approximate. However, at the electron temperatures $\sim 7000^\circ\text{K}$ as measured spectroscopically (Ref. 13) — and the degree of ionization ~ 0.01 as determined from macroscopic measurements (Ref. 18) — characteristic of this plasma, the calculated and measured conductivities are in the same range. This adds some assurance that the measurements reported herein are correct.

In aerodynamic applications, it is necessary to relate the electrical conductivity to the fluid properties of a supersonic flow. Thus knowledge of the region of the flow stream over which the electromagnetic field penetrates is important. In this case the region of plasma-field interaction is a hollow cylinder of plasma length only slightly greater than the coil length (2.6 cm) and 1 to 2 cm thick depending on the value of plasma conductivity. Since the fields decrease almost exponentially in the radial direction outward from the coil, the plasma affected most will be that of the first third of the penetration thickness. Aerodynamically, the gas in this region can be related to the free-stream conditions through standard aerodynamic treatment. Also, the effect of the boundary

layer on the probe walls must be evaluated for proper use of the data. Further treatment of these phenomena is not within the scope of this report.

SECTION V SUMMARY

In this report, a physical model for the coupling mechanism between an RF-excited coil and a conductive medium which surrounds the coil is established. From this model and using standard transformer techniques, the interaction between the coil and the conductive medium is explained in terms of the nondimensional parameter, Q_s . With the introduction of the parameter, Q_s , it becomes possible to relate ordinary circuit phenomena to electromagnetic field phenomena of the coil. The field phenomena interpretation of Q_s is used to show that, for a particular coil and excitation frequency, Q_s is a function only of the conductivity of the medium provided that $\sigma \gg \omega \epsilon$ (a provision which is readily satisfied for the media presented in this report). The circuit phenomena interpretation of Q_s is used to show that the change in plate voltage of a crystal-controlled oscillator due to the immersion of the coil in a conductive medium as contrasted to free space conditions is a function only of Q_s . Thus, it follows that the change in plate voltage is a function only of the conductivity of the media. The relationship between plate voltage and conductivity is obtained numerically by calibration techniques.

The important features of the circuit used in these conductivity measurements are: (1) the frequency is crystal-controlled, (2) the circuit and probe are simple both in design and analysis, (3) the plate voltage of the oscillator is the only measured quantity, and (4) the tests may be performed in short periods of time (~5 sec).

The primary difficulties associated with this method (as well as others) are that calibration procedures must be developed in order to relate the measured parameter (in this case, plate voltage) to conductivity. Additional difficulties arise since there are only two classes of materials, namely electrolytic solutions and semiconductors which have conductivities within the range of interest. Work is presently underway to further investigate calibration techniques using electrolytic solutions.

The measured values of conductivity in a d-c arc-generated supersonic plasma using the electrolytic calibration curve range from 70 to 280 mhos/meter. These measured values fall within the range of values calculated using a method suggested by Kantrowitz.

REFERENCES

1. Cambel, A. B. Plasma Physics and Magnetofluid Mechanics. McGraw-Hill Book Co., Inc., New York, 1963, Chapter 7.
2. Savic, P. and Boulton, G. T. "A Frequency Modulation Circuit for the Measurement of Gas Conductivity and Boundary Layer Thickness in a Shock Tube." National Research Council of Canada, MT43, May 1961.
3. Stock, F. T. and Baxter, D. C. "Tables of Reactance Integrals Relating to Eddy-Current Conductivity Probes." National Research Council of Canada, MK11, January 1963.
4. Marshall, T. and Hill, L. L. "A Radio-Frequency Technique for Determining the Electrical Conductivity of Ionized Gases." Paper presented at the Fifth United States Navy Symposium on Aeroballistics, White Oak, Maryland, October 1961.
5. Tanaka, H. and Hagi, M. "A Method of Measurement of Plasma Conductivity." Japanese Journal of Applied Physics, June 1964.
6. Kawashima, N. "Plasma Density Measurements by Use of FM Demodulators." Japanese Journal of Applied Physics, September 1964.
7. Poberzhskii, L. P. "Measurement of Electrical Conductivity of Gas Jets." Soviet Physics: Technical Physics, June 1964.
8. Olson, R. A. and Lary, E. C. "Conductivity Probe Measurements in Flames." AIAA Journal, Vol. 1, No. 11, November 1963.
9. Terman, F. E. Electronic and Radio Engineering. McGraw-Hill Book Company, Inc., New York, 1955. (Fourth Edition), Chapters 2 and 14.
10. Panofsky, W. K. H. and Phillips, M. Classical Electricity and Magnetism. Addison-Wesley Publishing Company, Inc., Reading, Massachusetts, 1962. (Second Edition).
11. Jackson, J. D. Classical Electrodynamics. John Wiley and Sons, Inc., New York, 1962.
12. Handbook of Chemistry and Physics. Chemical Rubber Publishing Co., (37th Edition), 1955-1956, p. 2369.
13. Brewer, L. E. "Spectroscopy of Supersonic Plasma, II. Excitation Temperature." AEDC-TDR-64-196 (AD447735), September 1964.

14. McGregor, W. K. and Brewer, L. E. "Spectroscopy of Supersonic Plasma, III. Electron Temperature Measurements in Argon Plasma by Two Independent Methods." AEDC-TR-65-131, November 1965.
15. Duclos, D. P. "The Equation of State of an Ionized Gas." AEDC-TN-60-192, October 1960.
16. Kantrowitz, A. R. and Petschek, H. E. Magnetohydrodynamics. Stanford University Press, Stanford, California, 1957.
17. Massey, H. S. W. and Burhop, E. H. S. Electronic and Ionic Impact Phenomena. Oxford University Press, 1952.
18. Bryson, R. J. and Fröhlich, J. P. "Study of the Energy Addition Process in a D-C Arc-Jet." AEDC-TR-65- (to be published).

APPENDIX I

HYDROMAGNETIC EFFECTS

The electromagnetic effects of a conductive fluid flowing with a velocity, \mathbf{v} , through a magnetic field are sometimes referred to as hydromagnetic effects. Thus, hydromagnetic effects occur when an RF-excited coil is immersed in a flowing ionized gas.

For an axially symmetric coil with an excitation frequency, $\omega = 3.142 \times 10^7 \text{ sec}^{-1}$, immersed in an axially flowing plasma, it will be shown that the hydromagnetic effects are negligible as compared to purely electromagnetic effects. Maxwell's equations for a linear, isotropic conductive medium moving with a velocity, \mathbf{v} , with respect to the coil are

$$\nabla \cdot \mathbf{E} = 0 \quad (\text{I-1})$$

$$\nabla \times \mathbf{E} = - \frac{\partial \mathbf{B}}{\partial t} \quad (\text{I-2})$$

$$\nabla \times \mathbf{B} = \mu \sigma (\mathbf{E} + \mathbf{v} \times \mathbf{B}) + \mu \epsilon \frac{\partial \mathbf{E}}{\partial t} \quad (\text{I-3})$$

$$\nabla \cdot \mathbf{B} = 0 \quad (\text{I-4})$$

Eliminating \mathbf{E} from Eq. (I-1) results in a wave equation for the magnetic field, \mathbf{B} . That is,

$$\left\{ \nabla^2 - \mu \sigma \frac{\partial}{\partial t} - \mu \epsilon \frac{\partial^2}{\partial t^2} \right\} \mathbf{B} = - \mu \sigma [\nabla \times (\mathbf{v} \times \mathbf{B})] \quad (\text{I-5})$$

Likewise, eliminating \mathbf{B} from Eq. (I-2) and assuming a steady-state flow field (i. e. $\frac{\partial \mathbf{v}}{\partial t} = 0$) gives a wave equation for the electric field, \mathbf{E} ,

$$\left\{ \nabla^2 - \mu \sigma \frac{\partial}{\partial t} - \mu \epsilon \frac{\partial^2}{\partial t^2} \right\} \mathbf{E} = - \mu \sigma [\mathbf{v} \times (\nabla \times \mathbf{E})] \quad (\text{I-6})$$

The terms $\nabla \times (\mathbf{v} \times \mathbf{B})$ and $\mathbf{v} \times (\nabla \times \mathbf{E})$ can be expanded into the form

$$\nabla \times (\mathbf{v} \times \mathbf{B}) = \mathbf{v} \nabla \cdot \mathbf{B} - \mathbf{B} \nabla \cdot \mathbf{v} = - \mathbf{B} (\nabla \cdot \mathbf{v}) \quad (\text{I-7})$$

$$\mathbf{v} \times (\nabla \times \mathbf{E}) = \nabla (\mathbf{v} \cdot \mathbf{E}) - \mathbf{E} \nabla \cdot \mathbf{v} \quad (\text{I-8})$$

For an axially symmetric coil and for an axially flowing fluid, $\mathbf{v} \cdot \mathbf{E} = 0$. Thus Eq. (I-8) becomes

$$\mathbf{v} \times (\nabla \times \mathbf{E}) = - \mathbf{E} (\nabla \cdot \mathbf{v}) \quad (\text{I-9})$$

Equations (I-5) and (I-6) may now be written in the form

$$\left\{ \nabla^2 - \mu \sigma \left[\frac{\partial}{\partial t} + \nabla \cdot \mathbf{v} \right] - \mu \epsilon \frac{\partial^2}{\partial t^2} \right\} \begin{Bmatrix} \mathbf{B} \\ \mathbf{E} \end{Bmatrix} = 0 \quad (\text{I-10})$$

The condition that the hydromagnetic effect be negligible is given by the inequalities

$$\left| \frac{\partial \mathbf{B}}{\partial t} \right| \gg |\mathbf{B} (\nabla \cdot \mathbf{v})| \quad (\text{I-11})$$

and

$$\left| \frac{\partial \mathbf{E}}{\partial t} \right| \gg |\mathbf{E} (\nabla \cdot \mathbf{v})| \quad (\text{I-12})$$

When the fields are varying sinusoidally in time with an angular frequency, ω , then the inequalities in Eqs. (I-11) and (I-12) reduce to

$$\omega \gg |\nabla \cdot \mathbf{v}| \quad (\text{I-13})$$

For axially flowing gases, $\nabla \cdot \mathbf{v} = \frac{\partial v}{\partial z}$ and when $\omega = 3.142 \times 10^7 \text{ sec}^{-1}$, Eq. (I-13) becomes

$$3.142 \times 10^7 \gg \left| \frac{\partial v}{\partial z} \right| \quad (\text{I-14})$$

Therefore, when this inequality is satisfied (which for all practical purposes is always true for aerodynamic flows), Eq. (I-10) becomes

$$\left\{ \nabla^2 - \mu \sigma \frac{\partial}{\partial t} - \mu \epsilon \frac{\partial^2}{\partial t^2} \right\} \begin{Bmatrix} \mathbf{B} \\ \mathbf{E} \end{Bmatrix} = 0 \quad (\text{I-15})$$

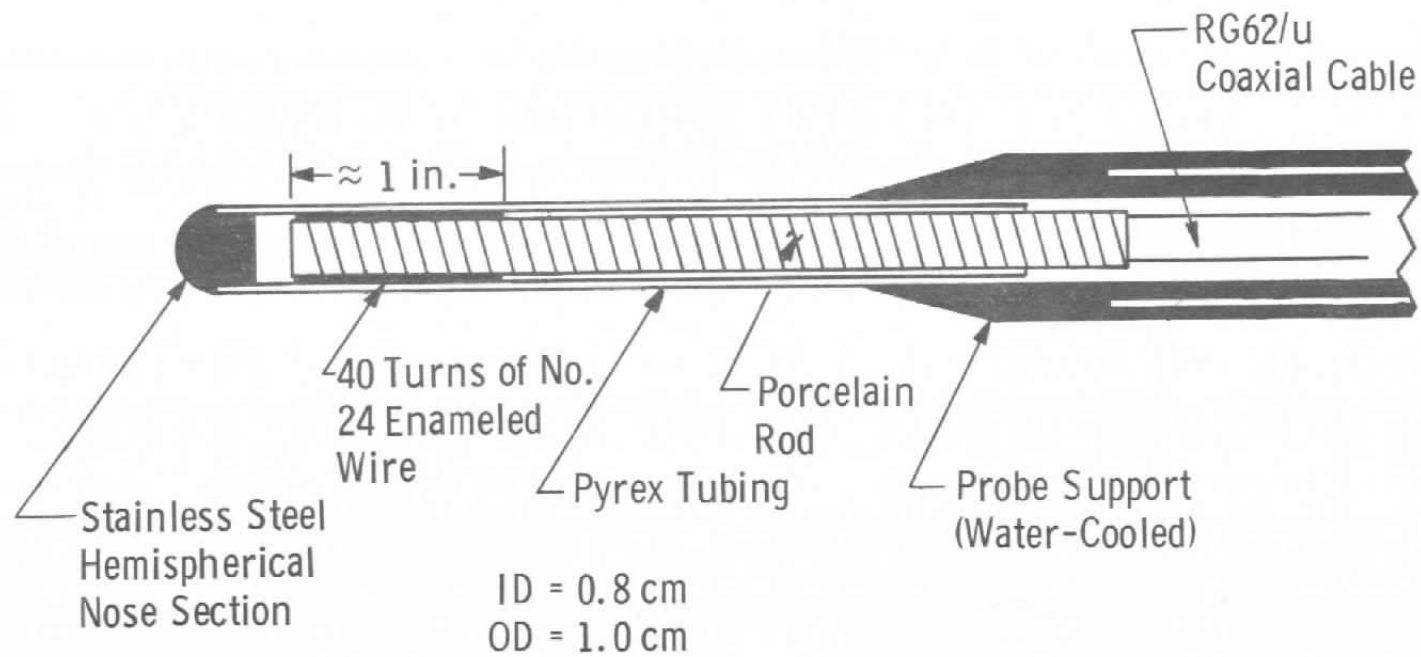
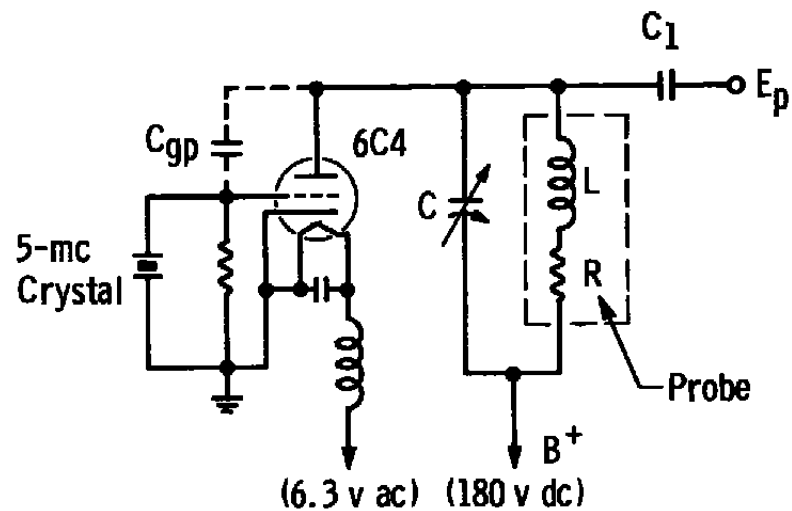


Fig. 1 Cross-Sectional View of Coil and Probe Support



a. Schematic Diagram of Crystal-Controlled Oscillator

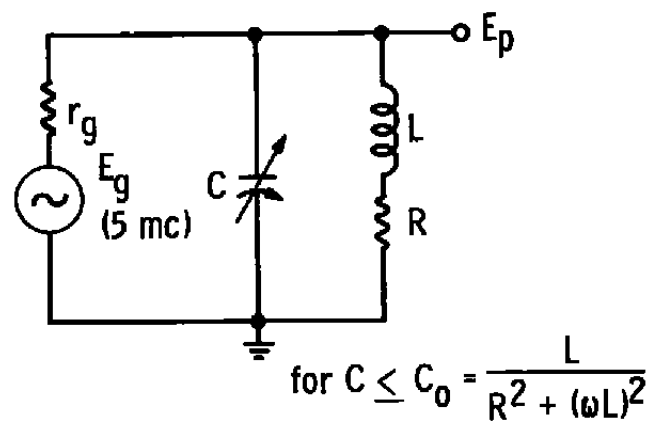
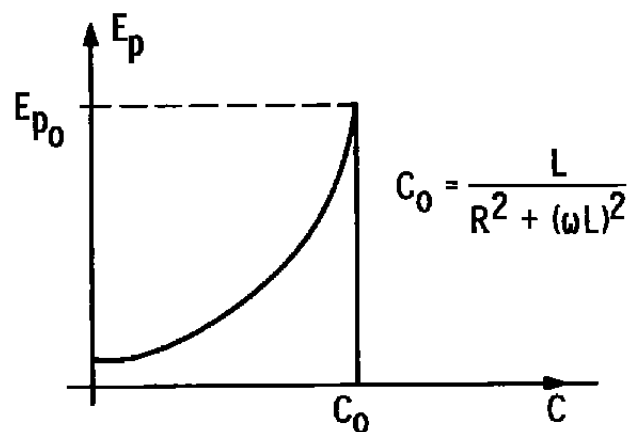
b. A-C Equivalent Circuit of Oscillator for $C \leq C_0$ c. Plate Voltage, E_p , versus Capacitance, C

Fig. 2 Oscillator and Probe

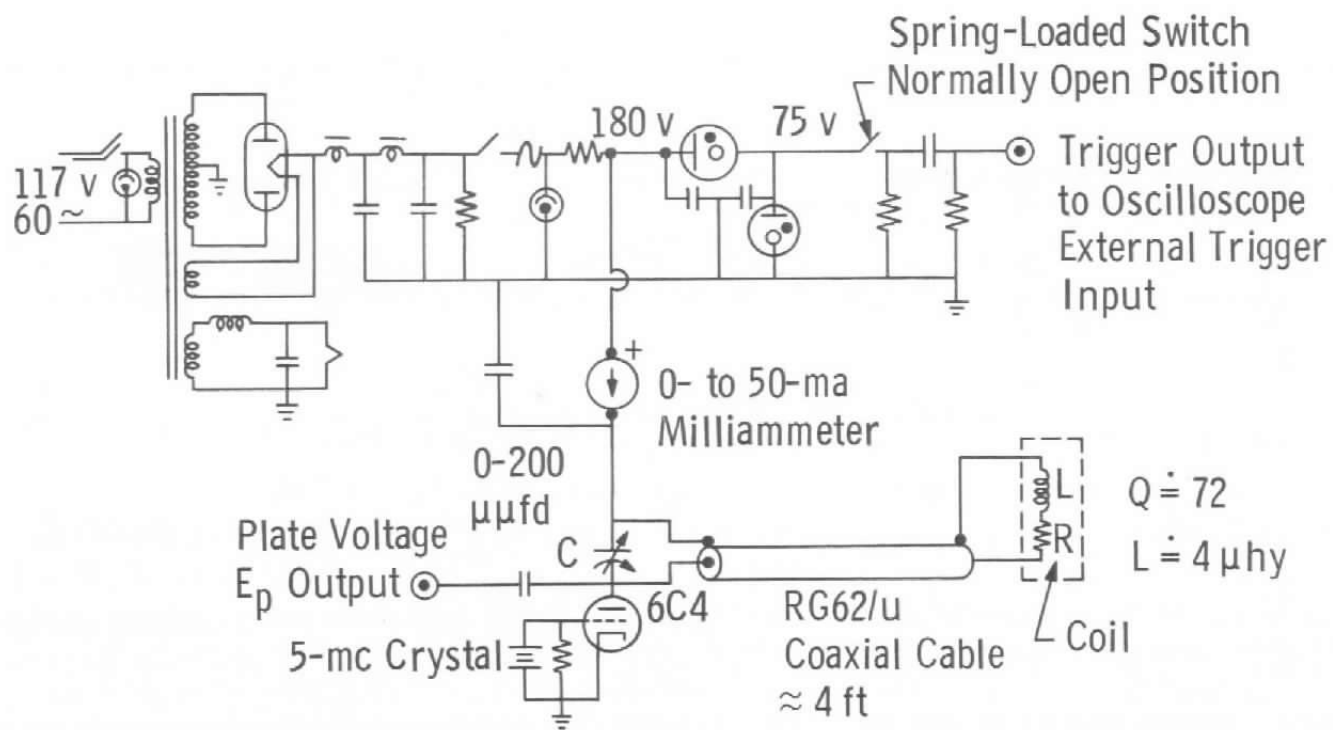
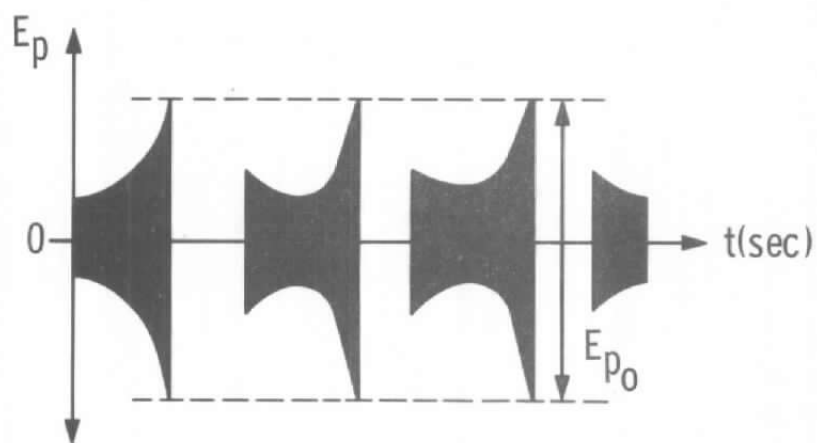


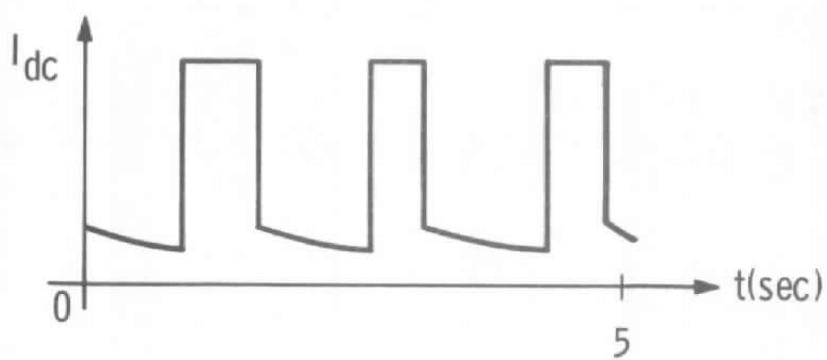
Fig. 3 Schematic Diagram of Electrical Circuit Including Power Supply and Triggering Unit



a. Recorded Output Voltage, E_p , (volts peak-to-peak)

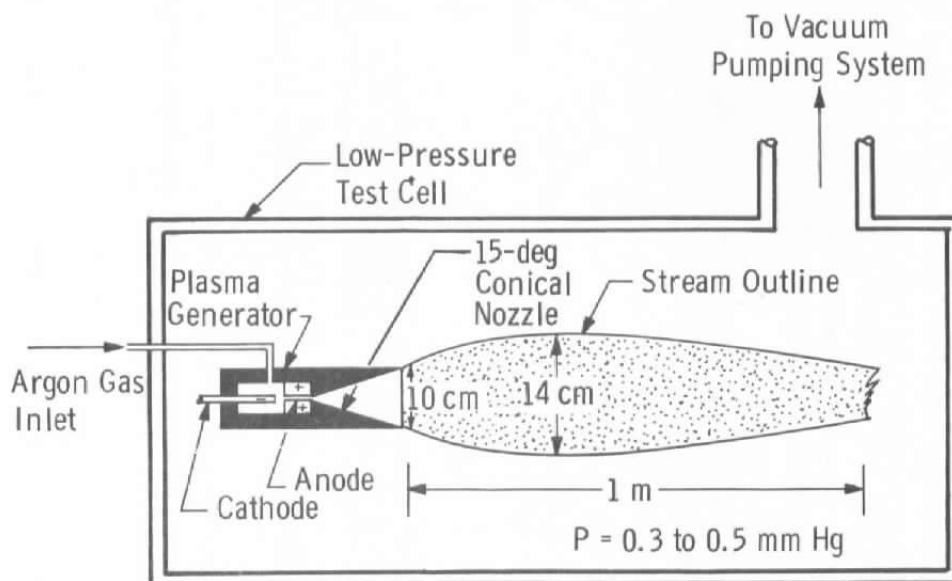


b. Capacitance, C ($\mu\mu\text{fd}$)

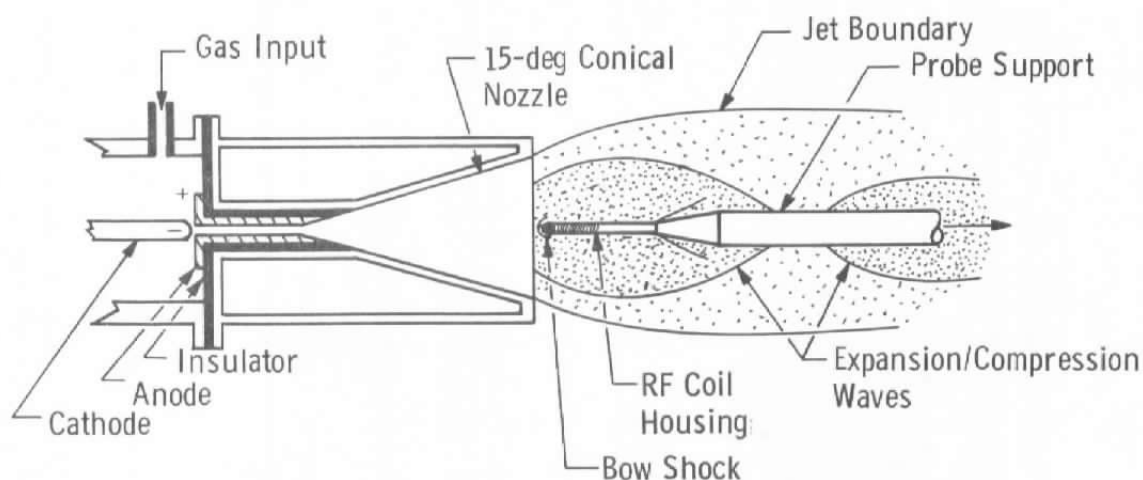


c. D-C Plate Current (ma)

Fig. 4 Oscillator Characteristics



a. Apparatus Schematic and Plasma Stream Characteristics



b. Free Jet Configuration with Dominant Flow Features Outlined

Fig. 5 Test Configurations

Northern Electric Co. - semiconductor mfg.
Battelle - up to electrolyte solutions?

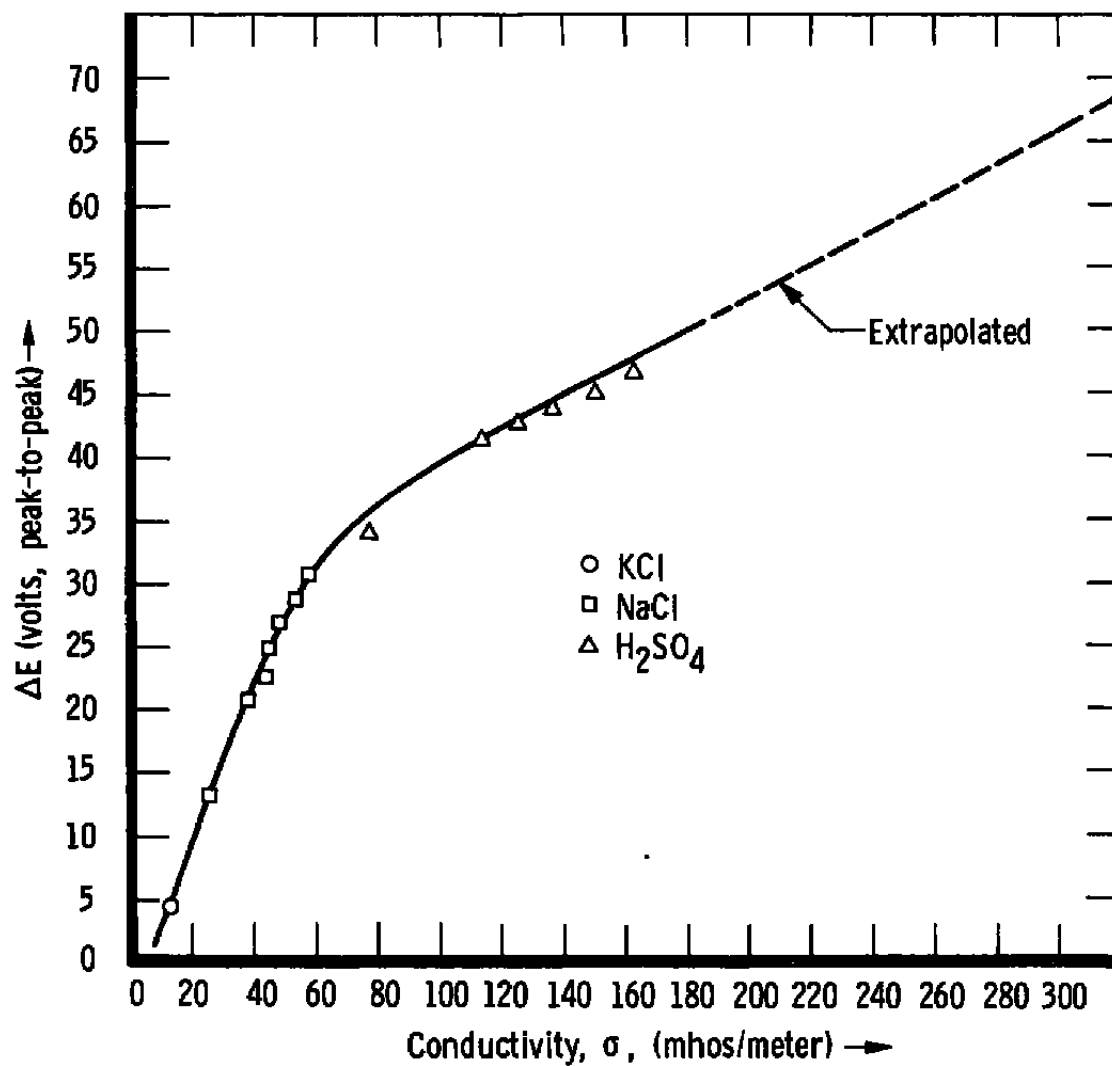


Fig. 6 Calibration Curve, ΔE (volts peak-to-peak) versus σ (mhos/meter)

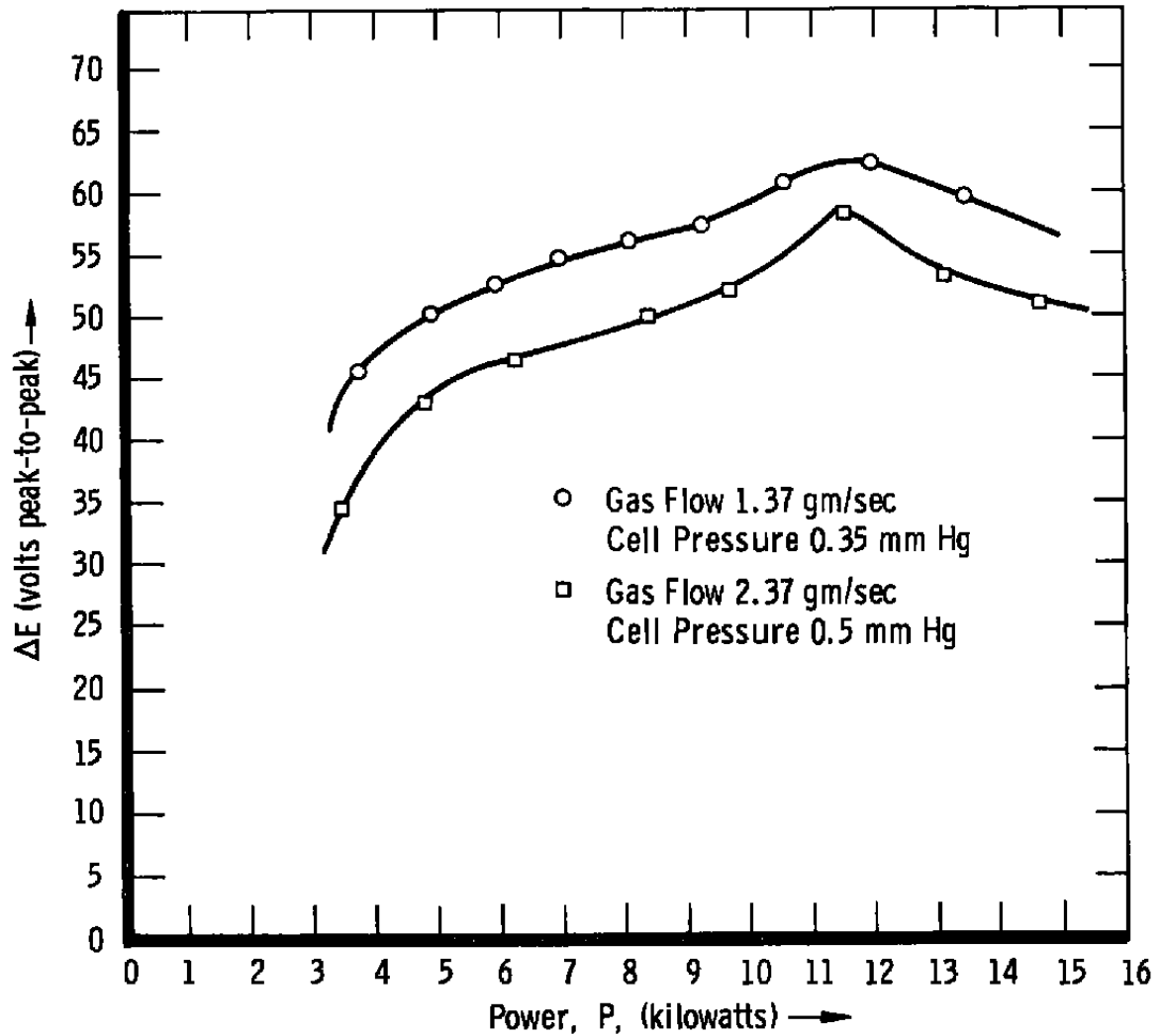


Fig. 7 Plot of ΔE (volts peak-to-peak) versus Plasma Generator Input Power, P (kilowatts)

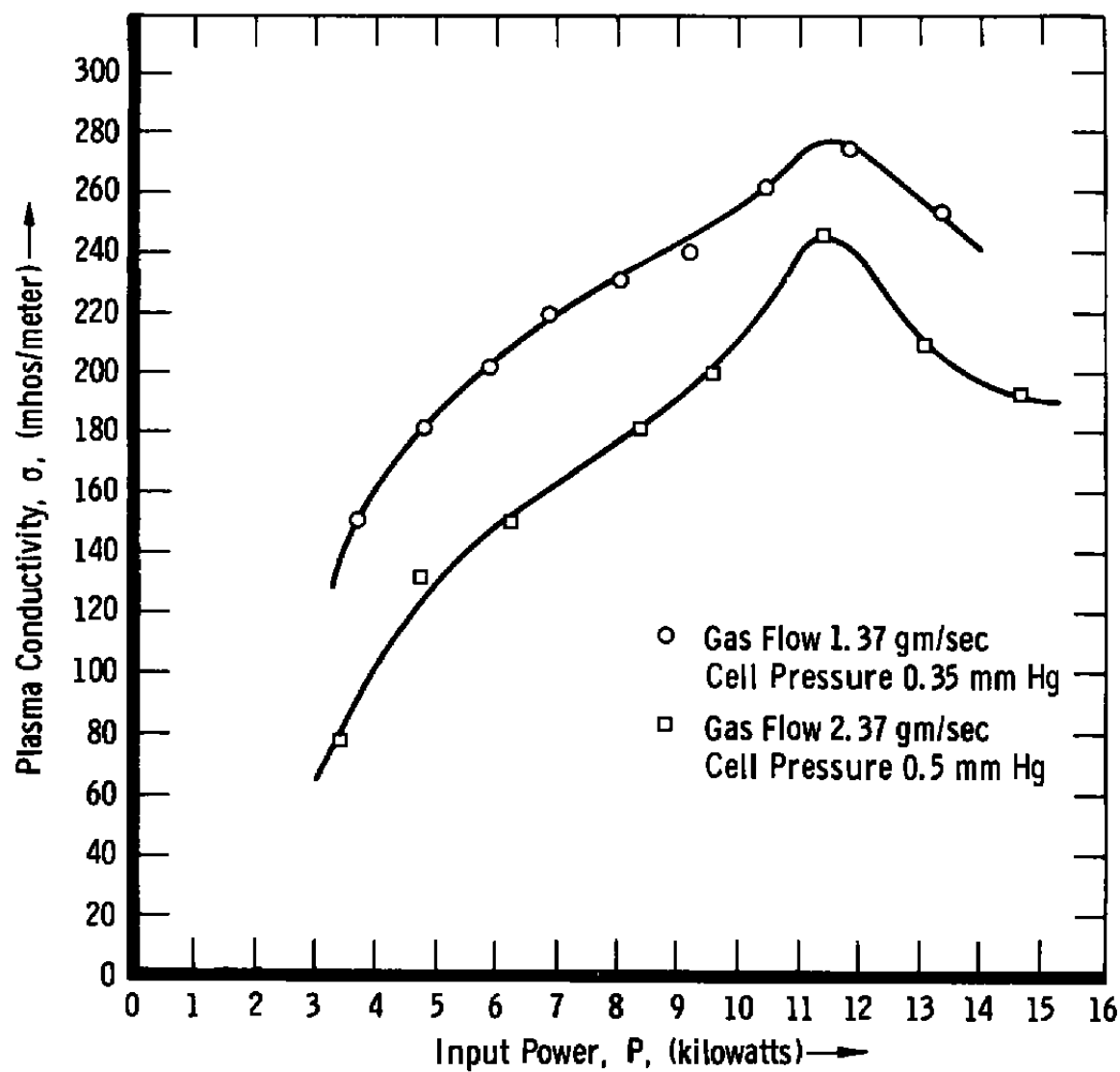


Fig. 8 Plot of Plasma Conductivity, σ (mhos/meter) versus Plasma Generator Input Power, P (kilowatts)

UNCLASSIFIED

Security Classification

DOCUMENT CONTROL DATA - R&D

(Security classification of title, body of abstract and indexing annotation must be entered when the overall report is classified)

1 ORIGINATING ACTIVITY (Corporate author) Arnold Engineering Development Center, ARO, Inc., Operating Contractor, Arnold Air Force Station, Tennessee		2a REPORT SECURITY CLASSIFICATION UNCLASSIFIED	
		2b GROUP N/A	
3 REPORT TITLE MEASUREMENT OF ELECTRICAL CONDUCTIVITY IN A LOW-DENSITY SUPERSONIC PLASMA			
4 DESCRIPTIVE NOTES (Type of report and inclusive dates) N/A			
5. AUTHOR(S) (Last name, first name, initial) Sprouse, J. A., ARO, Inc.			
6. REPORT DATE November 1965	7a TOTAL NO. OF PAGES 33	7b NO. OF REFS 18	
8a CONTRACT OR GRANT NO. AF40(600)-1200	9a. ORIGINATOR'S REPORT NUMBER(S) AEDC-TR-65-146		
b. PROJECT NO. 8951			
c Program Element 61445014	9b. OTHER REPORT NO(S) (Any other numbers that may be assigned this report)		
d Task 895101	N/A		
10. AVAILABILITY/LIMITATION NOTICES Qualified requesters may obtain copies of this report from DDC.			
11 SUPPLEMENTARY NOTES N/A	12. SPONSORING MILITARY ACTIVITY Arnold Engineering Development Center Air Force Systems Command, Arnold Air Force Station, Tennessee		
13 ABSTRACT Electrical conductivities in the range from 70 to 280 mhos/ meter were measured in an arc-heated, low-density, supersonic argon plasma. Measurements were made using a single layer coil acting as one branch of a tuned parallel circuit of a crystal- controlled oscillator operating at 5 mc/sec. Electromagnetic coupling between radio-frequency-excited coils and plasmas was examined, and the results are presented in terms of a nondimen- sional parameter, Q_s , which, for a particular coil, is a function only of the conductivity of the plasma surrounding the coil. Cal- culated conductivities using a combined form of the Spitzer-Härm and Chapman-Cowling equations for prescribed plasma conditions compare favorably with the measured results.			

14. KEY WORDS	LINK A		LINK B		LINK C	
	ROLE	WT	ROLE	WT	ROLE	WT
plasmas electrical conductivities supersonic flow low density arc heated plasma oscillations						

INSTRUCTIONS

1. **ORIGINATING ACTIVITY:** Enter the name and address of the contractor, subcontractor, grantee, Department of Defense activity or other organization (*corporate author*) issuing the report.

2a. **REPORT SECURITY CLASSIFICATION:** Enter the overall security classification of the report. Indicate whether "Restricted Data" is included. Marking is to be in accordance with appropriate security regulations.

2b. **GROUP:** Automatic downgrading is specified in DoD Directive 5200.10 and Armed Forces Industrial Manual. Enter the group number. Also, when applicable, show that optional markings have been used for Group 3 and Group 4 as authorized.

3. **REPORT TITLE:** Enter the complete report title in all capital letters. Titles in all cases should be unclassified. If a meaningful title cannot be selected without classification, show title classification in all capitals in parenthesis immediately following the title.

4. **DESCRIPTIVE NOTES:** If appropriate, enter the type of report, e.g., interim, progress, summary, annual, or final. Give the inclusive dates when a specific reporting period is covered.

5. **AUTHOR(S):** Enter the name(s) of author(s) as shown on or in the report. Enter last name, first name, middle initial. If military, show rank and branch of service. The name of the principal author is an absolute minimum requirement.

6. **REPORT DATE:** Enter the date of the report as day, month, year, or month, year. If more than one date appears on the report, use date of publication.

7a. **TOTAL NUMBER OF PAGES:** The total page count should follow normal pagination procedures, i.e., enter the number of pages containing information.

7b. **NUMBER OF REFERENCES:** Enter the total number of references cited in the report.

8a. **CONTRACT OR GRANT NUMBER:** If appropriate, enter the applicable number of the contract or grant under which the report was written.

8b, 8c, & 8d. **PROJECT NUMBER:** Enter the appropriate military department identification, such as project number, subproject number, system numbers, task number, etc.

9a. **ORIGINATOR'S REPORT NUMBER(S):** Enter the official report number by which the document will be identified and controlled by the originating activity. This number must be unique to this report.

9b. **OTHER REPORT NUMBER(S):** If the report has been assigned any other report numbers (*either by the originator or by the sponsor*), also enter this number(s).

10. **AVAILABILITY/LIMITATION NOTICES:** Enter any limitations on further dissemination of the report, other than those

imposed by security classification, using standard statements such as:

- (1) "Qualified requesters may obtain copies of this report from DDC."
- (2) "Foreign announcement and dissemination of this report by DDC is not authorized."
- (3) "U. S. Government agencies may obtain copies of this report directly from DDC. Other qualified DDC users shall request through _____."
- (4) "U. S. military agencies may obtain copies of this report directly from DDC. Other qualified users shall request through _____."
- (5) "All distribution of this report is controlled. Qualified DDC users shall request through _____."

If the report has been furnished to the Office of Technical Services, Department of Commerce, for sale to the public, indicate this fact and enter the price, if known.

11. **SUPPLEMENTARY NOTES:** Use for additional explanatory notes.

12. **SPONSORING MILITARY ACTIVITY:** Enter the name of the departmental project office or laboratory sponsoring (paying for) the research and development. Include address.

13. **ABSTRACT:** Enter an abstract giving a brief and factual summary of the document indicative of the report, even though it may also appear elsewhere in the body of the technical report. If additional space is required, a continuation sheet shall be attached.

It is highly desirable that the abstract of classified reports be unclassified. Each paragraph of the abstract shall end with an indication of the military security classification of the information in the paragraph, represented as (TS), (S), (C), or (U).

There is no limitation on the length of the abstract. However, the suggested length is from 150 to 225 words.

14. **KEY WORDS:** Key words are technically meaningful terms or short phrases that characterize a report and may be used as index entries for cataloging the report. Key words must be selected so that no security classification is required. Identifiers, such as equipment model designation, trade name, military project code name, geographic location, may be used as key words but will be followed by an indication of technical context. The assignment of links, rules, and weights is optional.